Journal of Alloys and Compounds 506 (2010) 492–495

Contents lists available at ScienceDirect

Journal of Alloys and Compounds

journal homepage: www.elsevier.com/locate/jallcom

Study of the *I–V* characteristics of SnO_2:F/$AgInS_2$ (p)/Al Schottky diodes

Z. Aissa, A. Bouzidi*, M. Amlouk

Unité de Physique de Dispositifs à Semiconducteurs – Faculté des Sciences de Tunis, Tunisia

ARTICLE INFO

Article history:
Received 8 April 2010
Received in revised form 2 July 2010
Accepted 8 July 2010
Available online 15 July 2010

Keywords:
$AgInS_2$
Chalcopyrite
Spray pyrolysis technique
I–V characteristics

ABSTRACT

$AgInS_2$ sprayed thin films have been deposited on glass SnO_2:F substrates using an aqueous solution which contains silver acetate ($AgCH_3CO_2$), thiourea ($SC(NH_2)_2$) and indium chloride ($InCl_3$) as precursors. The depositions were carried out at the substrate temperature of 420 °C. The concentration ratio in the spray solution of indium and silver elements $x = [Ag^+]/[In^{3+}]$ was equal to 1.3 whereas $y = [S^{2-}]/[In^{3+}]$ was varied between 5 and 7. The current–voltage study of SnO_2:F/$AgInS_2$/Al Shottky diodes as a function of *y* composition has been carried out. A rectifier effect has been shown and the transport process is mainly governed by the generation-recombination and tunneling effects.

1. Introduction

Silver indium disulfide $AgInS_2$ which belongs to I–II–VI_2 ternary compounds is an attractive material in possible photovoltaic and optoelectronic applications [1,2] because of its large absorption coefficient and its band gap energy lying in 1.87–2.03 eV domain [3,4]. During the last decade, the conversion efficiencies for polycrystalline CIGS based solar cells have been improved and the best cell is now reported close to 20% [5]. As a possible alternative, $AgInS_2$ based chalcopyrite semiconductor is also expected to make good solar cell absorber layer. This material has been prepared using different methods [6–9]. However, chemical deposition techniques have not been frequently used [10] to obtain this ternary compound which can crystallize in two forms: chalcopyrite and orthorhombic. Moreover, this compound could be obtained as n or p semiconductor type using appropriate experimental chemical conditions [11,12]. Recently, it is reported that $AgInS_2$ with p type conductivity has been obtained by introducing tin element Sn as dopant [13].

In this work, we report the *I*(*V*) characteristics of SnO_2:F/$AgInS_2$/Al diodes in which the silver indium disulfide thin films have been obtained by the spray pyrolysis technique using different concentration of sulfur in the starting solution.

To date, the *I*(*V*) study of such diodes based on p type $AgInS_2$ ternary semiconductor has not been tested.

2. Experimental

2.1. Film preparation

$AgInS_2$ thin films were obtained on 2 cm × 2 cm of SnO_2:F/glass substrates by spraying an aqueous solution containing silver acetate (CH_3COOAg), indium chloride ($InCl_3$) and thiourea ($SC(NH_2)_2$) as precursors. The substrate temperature Ts, of the order of 420 °C is used to prepare these films. The indium and silver concentrations were taken constant at 10^{-2} M and 1.3×10^{-2} M respectively whereas the concentration ratio of sulfur $y = [S^{2-}]/[In^{3+}]$ varied from 5 to 7. In our laboratory, successful deposition of crystalline $AgInS_2$ ternary compounds by the spray process was achieved thanks to a careful control of the spray temperature and solution composition [11,12]. The solution and gas flow rates were kept constant at 2 cm^3/min and 4 l/min respectively corresponding to a mini-spray pyrolysis. Nitrogen was used as the carrier gas to avoid chemisorptions of oxygen.

2.2. Characterization techniques

First, film surfaces were analyzed by atomic force microscopy (AFM) (VEECO digital instrument 3A) in contact mode.

Second, for resistivity measurements, an electrometer Keithley 230 programmable voltage source 230 was used to measure the film's resistivity at room temperature and the type character for the film was found using the hot probe method.

To test $AgInS_2$ (p) sprayed thin films as absorbers in expected possible photovoltaic solar cells in our laboratory, it seems necessary to understand their electrical properties. For this purpose, the mechanisms of conduction of $AgInS_2$ (p)/Al Schottky structures have been developed. The analysis of electrical junctions requires an ohmic contact on the side of the semiconductor $AgInS_2$ (p). 0.5 μm thick sprayed tin oxide SnO_2 doped with fluorine (F) (SnO_2:F (FTO)) has chosen as substrate [14].

Finally, Al evaporated thin film (700 Å) is used as front contact while a conductive oxide-coated glasses SnO_2:F with mean resistance value of the order of 10 Ω were used as back contact electrode. In the same line, *I–V* data collection was made by using the same electrometer and LabView data acquisition software. The active area of these diodes was 1 cm^2. The schematic drawing of the diode is presented in Fig. 1.

* Corresponding author. Tel.: +216 71 872 600; fax: +216 71 885 073.
E-mail address: abdellatif.bouzidi@isi.rnu.tn (A. Bouzidi).

0925-8388/$ – see front matter © 2010 Elsevier B.V. All rights reserved.
doi:10.1016/j.jallcom.2010.07.053

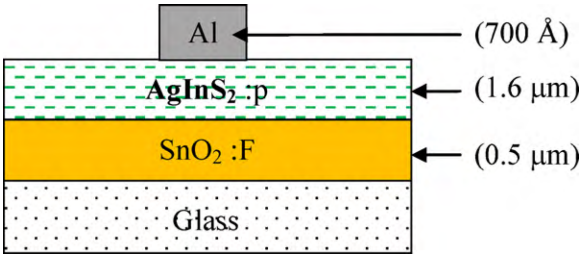

Fig. 1. Schematic drawing of SnO_2:F/$AgInS_2$/Al Schottky diode.

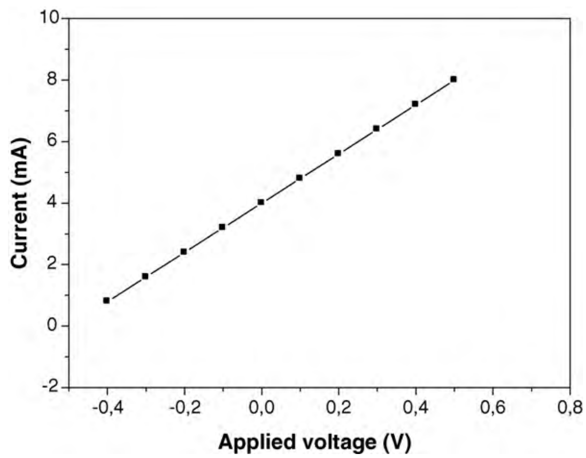

Fig. 2. Ohmic contact of SnO_2 (F)/$AgInS_2$/Au for $y = 5$.

3. Results and discussion

3.1. SnO_2 (F)/$AgInS_2$ (p) contact

To ensure the ohmic nature of SnO_2 (F)/$AgInS_2$ (p) contact, a gold film evaporated directly on $AgInS_2$ (p) side. This film acts as a second electrode for this test. As shown in Fig. 2, the curve $I(V)$ the structure of SnO_2 (F)/$AgInS_2$ (p)/Au exhibits a good linearity which confirms that SnO_2/$AgInS_2$ contact is ohmic.

3.2. Resistivity and morphology

Fig. 3 depicts the resistivity values of spayed $AgInS_2$ films using various concentration ratios y (5, 6 and 7). All films prepared with these concentration ratios and having 1.6 µm as thickness, exhibits p semiconductor type character. We note firstly an increase in the resistivity when y increases which may be due to the excess in sulfur element leading to the formation of Ag_2S [13]. The presence of undesirable secondary phase, as a function of the composition, is also reported by other authors using different experimental conditions [4,15]. Thus, the resistivity remains higher than 10^3 Ω cm when the ratio y is equal to 7.

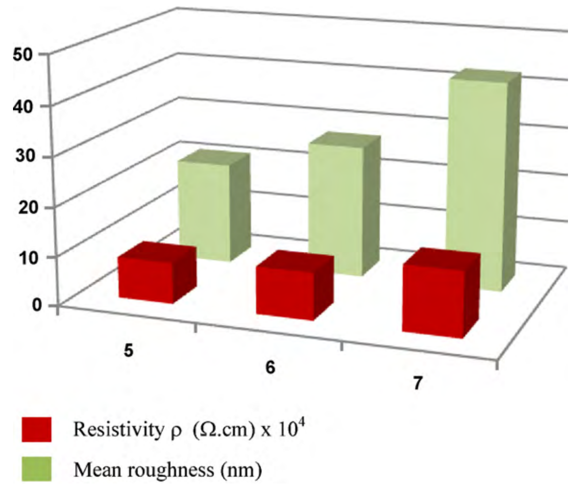

Fig. 3. Resistivity and roughness measurements as a function of the concentration ratio y.

Table 1
V_d values in terms of the concentration ratio y.

y	5	6	7
V_d (V)	0.50	0.52	0.54

2D AFM micrographs, shown in Fig. 4, reveal that all $AgInS_2$ films surfaces are rough. These perturbed surfaces are probably due to very small droplets resulting from the mini-spray pyrolysis technique that vaporize above the glass substrates and condense as micro-crystallites with various sizes. Indeed, for sample prepared at $y = 5$ and 6 we have rounded clusters and the roughness parameter increases when the sulfur composition increases in the spray solution, Fig. 3. This phenomenon may be due to sulfur excess in solid phase. Indeed, as far as the composition increases, the presence of Ag_2S secondary phase becomes visible in $AgInS_2$ thin film as shown in X-ray diffraction (XRD) study reported previously [13].

3.3. I–V characteristics simulation based on double diode model

The experimental forward and reverse bias $I(V)$ characteristics of SnO_2/$AgInS_2$/Al Schottky diodes at room temperature are shown in Fig. 5.

These characteristics reveal clearly the rectifier behavior for all these junctions characterized by a diffusion potential V_d having an average value of 0.52 V, Table 1.

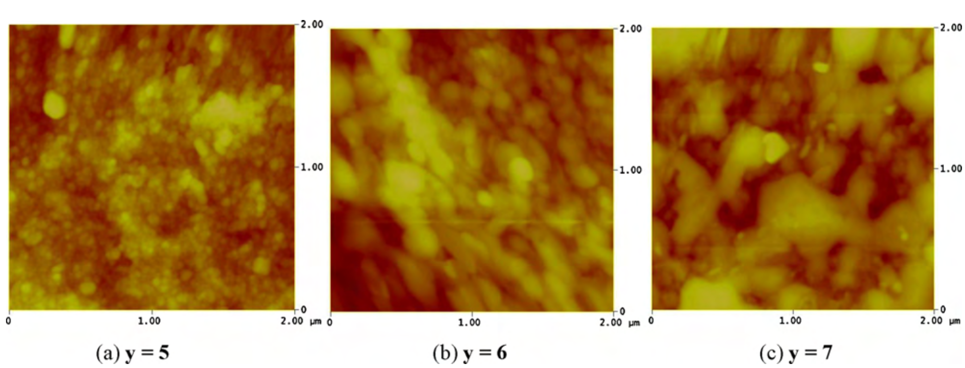

Fig. 4. 2D AFM micrographs of the sprayed $AgInS_2$ films corresponding to different concentration ratio of sulfur $y = [S^{2-}]/[In^{3+}]$: $y = 5$ (a), $y = 6$ (b) and $y = 7$ (c).

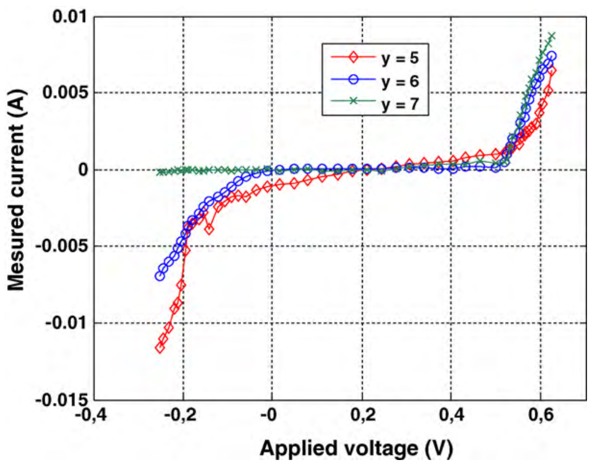

Fig. 5. The experimental forward and reverse bias $I(V)$ characteristics of Schottky contacts $SnO_2/AgInS_2/Al$ for various y.

In this section, the double exponential physical parameters of $AgInS_2/Al$ junction have been extracted using Matlab software by simulating the $I(V)$ characteristics.

The $I(V)$ characteristic of such junctions can be written as an implicit equation:

$$I=I_{01}\left(\exp\left(\frac{V-R_SI}{V_T}\right)-1\right)+I_{02}\left(\exp\left(\frac{V-R_SI}{AV_T}-1\right)\right)+\frac{V-R_SI}{R_{sh}} \quad (1)$$

where $V_T = kT/q$ is the thermal voltage, A is the junction quality factor related to the recombination processes, R_s and R_{sh} are the series and the shunt resistances respectively in the equivalent circuit, I_{01} and I_{02} are the diode reverse saturation currents. I_{01} is the current generated in the bulk of the junction and I_{02} is rather the recombination one.

These five physical junction parameters R_s, R_{sh}, I_{01}, I_{02} and A are calculated from the current–voltage measured characteristics in such way that the simulated $I–V$ characteristic of the diode is as close as possible to the measured one. The difference between the two curves is calculated as a simulation quality factor (SQF) using the last square method.

First, the series resistance R_s is determined by linear fitting of $I(dI/dV) = f(I)$, and its value is equal to 2.48 Ω for diode using $y = 5$.

Second, the shunt resistance R_{sh} is deduced by $R_{sh} = (dV/dI)$ near zero, which gives $R_{sh} = 1000\ \Omega$ for $y = 5$.

After that, and for each value of A and D, $I_2 = I_{02}\exp((V - R_sI)/AV_T)$ current value is determinate as a solution of the Newton equation:

$$I-\frac{V-R_sI}{R_{sh}}=I_2+D.I_2^A \quad (2)$$

Then we calculated:

$$f(I)=V-V_T\cdot\ln(I_2^A) \quad (3)$$

which is linear when A and D correspond to the Eq. (1): $f(I) = R_sI + b$.

The saturation currents I_{01}, I_{02} are then obtained as follows:

$$I_{02}=\exp\left(\frac{-b}{V_TA}\right)\quad\text{and}\quad I_{01}=DI_{02}^A \quad (4)$$

Finally, these parameters (R_s, R_{sh}, I_{01}, I_{02} and A) where replaced in Eq. (1) and the simulation quality factor SQF has been calculate using: $SQF=\left(\sum d_i^2\right)^{1/2}$; where d_i is the distance between the simulated points and the measured ones from positive experimental $I–V$ characteristic. N is the number of points.

The lowest SQF corresponds to the best values of the junction parameters model. This simulation gives SQF equal 0.133×10^{-4} for samples with $y = 5$ corresponding to values: $A = 2$, $R_s = 2.480\ \Omega$, $R_{sh} = 1000\ \Omega$, $I_{01} = 1.3753 \times 10^{-13}$ A and $I_{02} = 9.2714 \times 10^{-8}$ A.

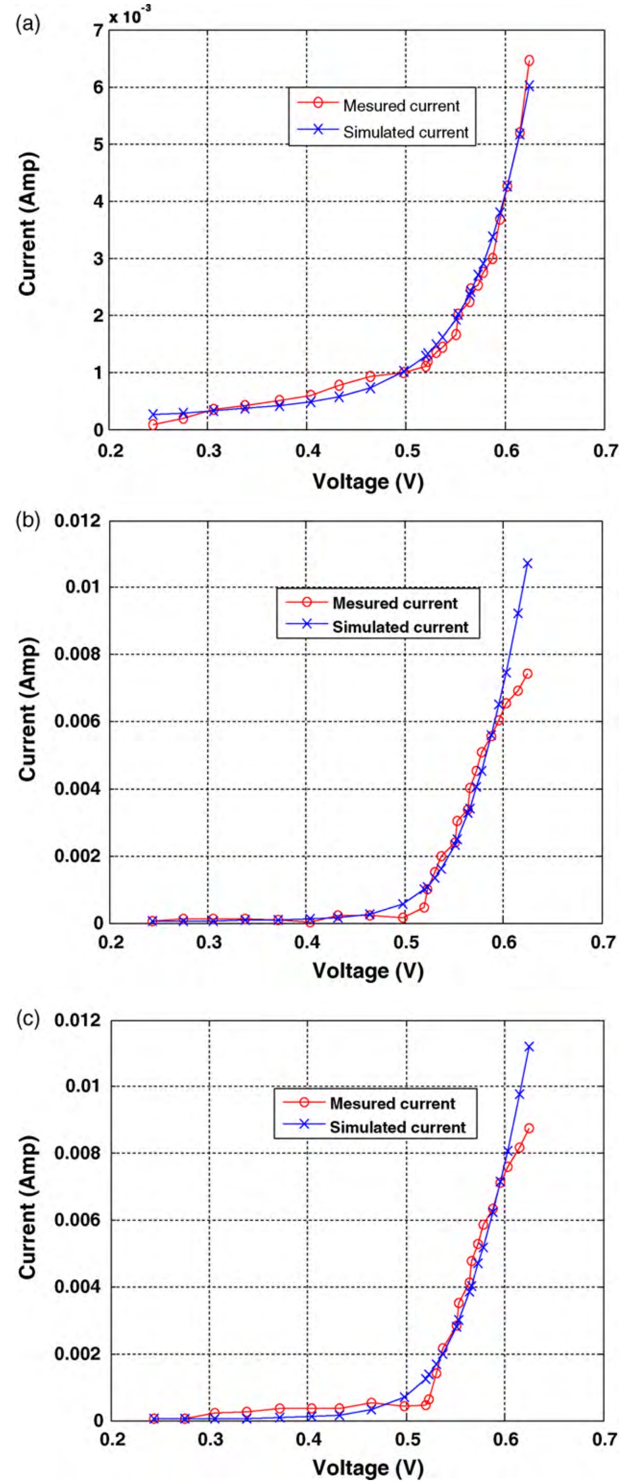

Fig. 6. The measured and simulated $I(V)$ characteristics of $AgInS_2/Al$ corresponding to $y = 5$ (a), $y = 6$ (b) and $y = 7$ (c).

Fig. 6 gives the $I(V)$ measured and simulated characteristics of $AgInS_2/Al$ structures for various concentration ratio y.

In Table 2 the $I(V)$ calculated performances of these diodes in terms of the y composition are summarized.

As seen in Table 2 and Fig. 5, good simulated $I–V$ characteristics corresponding to SQF as lower as 10^{-4} is obtained for $AgInS_2/Al$

Table 2
SnO_2:F/$AgInS_2$/Ag diodes calculated parameters as a function of the concentration ratio *y*.

$AgInS_2$ samples	Q_{min}	A	R_s (Ω)	R_{sh} (Ω)	I_{01} (pA)	I_{02} (nA)
$y=5$	0.13×10^{-4}	2	2.5	1000	13.7	92.7
$y=6$	4.68×10^{-4}	2.01	3.7	5100	3.9	27.1
$y=7$	4.58×10^{-4}	2.04	4.2	6200	5.4	46.3

Schottky diode prepared using $y=5$. This result is consistent with AFM morphology and resistivity studies described above.

It is noted that, in an ideal case R_s should be zero and R_{sh} should be infinite to get 100% fill factor. In general, R_s and R_{sh} depend on metal contact nature and bulk defaults respectively. Although, R_{sh} value of $AgInS_2$/Al diode prepared using $y=6$ and $y=7$ are higher than R_{sh} corresponding to $y=5$ one, and an avalanche effect has been observed for this diode showing the presence of un-negligible defaults in bulk which can be explained by the presence of sulfur excess. The magnitude of R_{sh} and R_s is influenced by chemical composition as well as the morphology of the $AgInS_2$ sprayed thin films. Moreover, changes in the front and back contacts can further influence R_{sh} and R_s values.

For all diodes prepared at various concentration *y*, the ideality factor *A* is higher than 2. In the same way, I_{02} values are so greater than I_{01} ones. These results show that the electrical transport process is governed by the generation-recombination and tunneling effects.

4. Conclusion

Based on the electrical current–voltage *I*–*V*, the electrical parameters of SnO_2:F/$AgInS_2$/Al Schottky diodes have been achieved using the double exponential model. The series resistance R_s is low for all diodes ($R_s < 5$ Ω) whereas the shunt resistance R_{sh} is greater than 1 kΩ. On the other hand, the ideality factor *A* of the diode is greater than 2 indicating that the transport process is governed by the generation-recombination and tunneling effects. This study seems to be attractive since photovoltaic solar cells with $AgInS_2$-absorbers could be tested.

References

[1] M.L. Albor-Aguilera, D. Ramírez-Rosales, M.A. González-Trujillo, Thin Solid Films 517 (February (7)) (2009) 2535–2537.
[2] K.J. Hong, et al., Journal of Physics and Chemistry of Solids 64 (July (7)) (2003) 1119–1124.
[3] K.J. Hong, J. WJeong, T.S. Jeoong, C.J. Youn, W.S. Lee, J.S. Park, D.C. Shin., Journal of Physics and Chemistry of Solids 64 (2003) 1119.
[4] M. Ortega-Lopez, O. Vigil-Galan, F. Cruz Gandarilla, O. Solorza-Feria, Materials Research Bulletin 38 (2003) 55.
[5] M.A. Contreras, K. Ramanathan, J. AbuShama, F. Hasoon, D.L. Young, B. Egaas, R. Noufi, Progress in Photovoltaics Research and Application 13 (2005) 209.
[6] K. Yoshino, H. Komaki, T. Kakeno, Y. Akaki, T. Ikari, Journal of Physics and Chemistry of Solids 64 (2003) 1839.
[7] G. Delgado, A.J. Mora, C. Pineda, T. Tinoco, Materials Research Bulletin 36 (2001) 2507.
[8] K. Yoshino, N. Mitani, M. Sugiyama, S.F. Chichibu, H. Komaki, T. Ikari, Physica B 302–303 (2001) 349.
[9] S.H. Youa, K.J. Lee, T.S. Jeong, C.J. Youn, J.S. Park, S.N. Baek, J. Cryst. Growth 245 (2002) 261.
[10] M. Gorsca, R. Beaulieu, J.J. Loferski, B. Roessler, Thin Solid Films 67 (1980) 341.
[11] Z. Aissa, T. Ben Nasrallah, M. Amlouk, J.C. Bernède, S. Belgacem, Solar Energy Materials & Solar Cells 90 (2006) 1136–1146.
[12] Z. Aissa, M. Amlouk, T. Ben Nasrallah, J.C. Bernède, S. Belgacem, Solar Energy Materials & Solar Cells 91 (2007) 489–494.
[13] M.L. Albor-Aguilera, D. Ramirez-Rasales, M.A. Gonzalez-Trujillo, Thin Solid Films 517 (2009) 2535–2537.
[14] M. Amlouk, M. Dachraoui, S. Belgacem, R. Bennaceur, Solar Energy Materials 15 (1987) 453–461.
[15] M. Ortega-Lopez, A. Morales-Acevedo, O. Solorza-Feria, Thin Solid Films 385 (2001) 120.